

## Evidence for nanoindentation-induced phase transformations in germanium

Jae-il Jang

*Department of Materials Science and Engineering, The University of Tennessee, Knoxville, Tennessee 37996-2200*

M. J. Lance

*Oak Ridge National Laboratory, Metals and Ceramics Division, Oak Ridge, Tennessee 37831*

Songqing Wen and G. M. Pharr<sup>a)</sup>

*Department of Materials Science and Engineering, The University of Tennessee, Knoxville, Tennessee 37996-2200*

(Received 18 November 2004; accepted 11 February 2005; published online 21 March 2005)

Nanoindentation experiments were performed using Berkovich and cube-corner indenters to investigate whether nanoindentation-induced phase transformations, such as those observed in silicon, also occur in germanium. Although the indentation load-displacement curves for germanium do not show the unloading pop-out or elbow phenomena observed in silicon, clear evidence for phase transformations was obtained by scanning electron microscopy (SEM) and micro-Raman spectroscopy. SEM showed that there is extruded material around the contact periphery of cube-corner hardness impressions that is metalliclike in its flow characteristics, just as in silicon. Micro-Raman spectroscopy revealed more direct evidence by identifying amorphous and what may be the crystalline BC8 (Ge-IV) phase. The fact that these phenomena are observed primarily and reproducibly only for the cube-corner indenter suggests that the contact geometry significantly affects the transformation behavior. Results are discussed in terms of possible deformation mechanisms and how they may be influenced by the indenter geometry. © 2005 American Institute of Physics. [DOI: 10.1063/1.1894588]

High-pressure experiments conducted over the past four decades<sup>1-5</sup> have shown that under hydrostatic loading conditions at room temperature, the Ge-I diamond cubic structure transforms to the metallic  $\beta$ -tin structure (Ge-II) at a pressure of about 10–11 GPa. Upon unloading, two different metastable crystalline phases can form depending on the unloading rate. For slow unloading, the Ge-II phase transforms to the simple tetragonal Ge-III (ST12 structure), but for fast unloading the predominant phase is the body-centered-cubic Ge-IV phase (BC8 structure).

Since these transformations are broadly analogous to those occurring in silicon, one might expect that the widely reported indentation-induced phase transformations in silicon<sup>6</sup> would also be observed in Ge. However, as noted by Domnich and Gogotsi in their recent review article,<sup>6</sup> although there is some evidence for phase transformations for higher load indentations made with a Vickers indenter,<sup>7-9</sup> there is little reproducible evidence that the transformations occur during nanoindentation. In particular, Raman peaks for transformed phases have not been observed reproducibly in nanoindentations,<sup>10,11</sup> and a recent cross-sectional transmission electron microscopy study<sup>11</sup> has shown that severe twinning, rather than phase transformation, is the primary mechanism of deformation in Ge during spherical indentation. The purpose of this letter is to report observations that show that phase transformations do indeed occur during nanoindentation of germanium.

Nanoindentations were made on a standard (100) Ge wafer using a Nanoindenter-XP (MTS System Corp., Oak

Ridge, TN). Two triangular pyramidal indenters with centerline-to-face angles of 35.3° (cube-corner indenter) and 65.3° (Berkovich indenter) were employed in a manner similar to a recent study of silicon.<sup>12</sup> Most tests were performed to a peak load of 50 mN at loading/unloading rates of 0.5 and 5 mN/s. Micro-Raman analyses of the hardness impressions were conducted within 1 h of nanoindentation using a Dilor XY800 Microprobe (JY Inc., Edison, NJ) to identify transformed phases. To examine the stability of these phases, they were also examined one and two days later. An Ar<sup>+</sup> laser operating at 5145 Å was focused to a spot size of approximately 1  $\mu$ m on the sample, and the light collected back into the microscope was dispersed with a diffraction grating and detected with a charge-coupled device detector. The beam intensity was kept low to minimize possible artifacts caused by laser heating. Subsequent to the micro-Raman measurements, the hardness impressions were imaged using a Leo 1525 field-emission scanning electron microscopy (SEM, Carl Zeiss SMT Inc, Thornwood, NY) to identify important topographical features of the hardness impressions.

Figure 1 shows typical nanoindentation load-displacement ( $P$ - $h$ ) curves observed in the study. The sharper cube-corner indenter produces a larger peak-load displacement and a greater proportion of permanent plastic deformation after unloading than the Berkovich indenter. The cube-corner indenter also produces a number of displacement discontinuities in the loading curve which are caused by discontinuous crack extension and chipping. With a fracture toughness of about half that of silicon,<sup>13</sup> germanium is much more brittle and cracking is thus much more extensive. In comparison to silicon, the most noteworthy feature in the  $P$ - $h$  curves is the lack of a “pop-out” or an “elbow” in the

<sup>a)</sup>Also at: Oak Ridge National Laboratory, Metals and Ceramics Division, Oak Ridge, Tennessee 37831; electronic mail: pharr@utk.edu

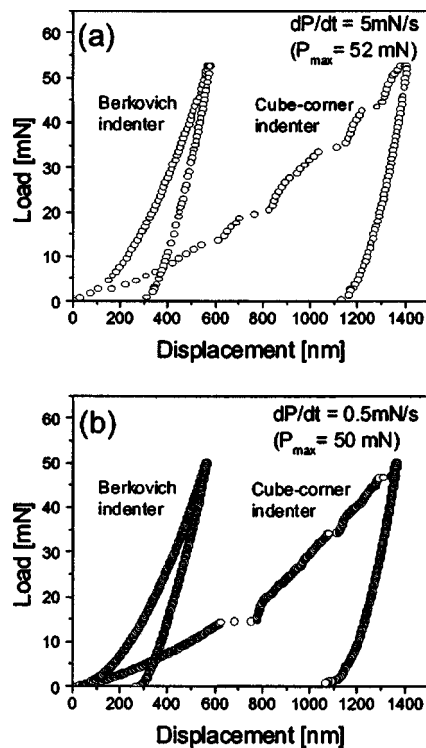


FIG. 1. Nanoindentation load-displacement curves made with cube-corner and Berkovich indenters to a peak load  $P_{\text{max}}=50 \text{ mN}$ : (a)  $dP/dt=5 \text{ mN/s}$ , and (b)  $dP/dt=0.5 \text{ mN/s}$ .

unloading curve for indentations made with the Berkovich indenter.<sup>6,12</sup> The pop-out and elbow phenomena observed in Si are usually associated with transformation from high pressure Si-II phase to metastable crystalline phases (Si-III and Si-XII) and amorphous Si, respectively. As shown in Fig. 1, neither of these features nor anything like them is observed in germanium. The unloading curves have the normal appearance of elastic recovery.

Although the  $P$ - $h$  curves show no evidence for a phase transformation, SEM observation of the cube-corner hardness impressions, as shown in Figs. 2(a) and 2(b), revealed a thin layer of extruded material around the entire contact periphery. As in the case of silicon,<sup>14</sup> this extrusion indicates that a soft ductile phase that can flow like a metal (e.g., Ge-II) is sandwiched between the diamond indenter and the relatively hard surrounding Ge-I. While the extrusion behavior is well known only in Si,<sup>14</sup> this is a clear observation of the phenomena in Ge. In contrast to the cube-corner indentations, the Berkovich indentations shown in Figs. 2(c) and 2(d) exhibited no extrusion, although close inspection reveals that there is a zone of what appears to be severely deformed material inside the contact impression that gives it a mottled rather than smooth appearance. Hainsworth *et al.*<sup>15</sup> first observed these zones (they called them “extruded layers”) and attributed them to plastic deformation and extrusion of the metallic Ge-II phase in the same way it occurs in Si.<sup>14</sup> However, because the material does not extend beyond the edge of the hardness impression, it is difficult to conclude whether it is formed in response to a metallic phase transformation or to highly constrained plastic flow.

Additional evidence for indentation-induced phase transformations was obtained through micro-Raman spectroscopy. Figure 3(a) presents micro-Raman spectra for cube-corner indentations made at the faster loading rate of  $5 \text{ mN/s}$ . Four

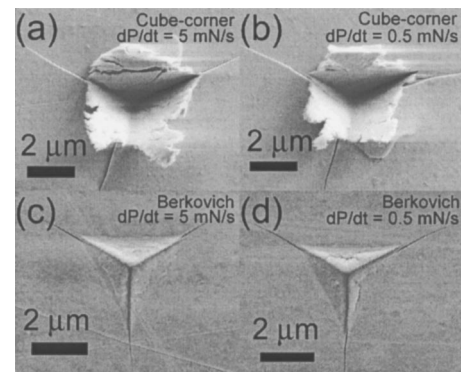


FIG. 2. SEM micrographs of nanoindentations made at  $P_{\text{max}}=50 \text{ mN}$ : (a) Cube-corner indenter,  $dP/dt=5 \text{ mN/s}$ , (b) cube-corner indenter,  $dP/dt=0.5 \text{ mN/s}$ , (c) Berkovich indenter,  $dP/dt=5 \text{ mN/s}$ , and (d) Berkovich indenter,  $dP/dt=0.5 \text{ mN/s}$ . Note that the magnifications for the micrographs are slightly different.

spectra are shown—one before indentation and three others at times of 1, 20, and 44 h after indentation. Although the pristine Ge-I shows only one peak at  $300 \text{ cm}^{-1}$ , the material examined 1 h after indentation exhibits distinct narrow peaks at  $205, 230, 250,$  and  $264 \text{ cm}^{-1}$  and broad bands around  $150$  and  $270 \text{ cm}^{-1}$ . The broad bands have been identified as amorphous Ge.<sup>9</sup> The narrow crystalline peaks between  $200$  and  $270 \text{ cm}^{-1}$  are different from the observed peaks for ST12-Ge (Ge-III) phase,<sup>2</sup> but are very similar to peaks observed in diamond anvil cell experiments by Hanfland and Syassen,<sup>3</sup> who pointed out their striking similarity to BC8-Si (Si-III). Based on this observation and the fact that faster unloading rates promote the transformation to the BC8-Ge (Ge-IV) phase in diamond anvil cell studies,<sup>6</sup> we tentatively assign these peaks to Ge-IV, but note that confirmed Raman spectra for this phase are not yet available. Gogotsi *et al.* also observed peaks like these in Berkovich indentations made at an unspecified “high” loading rate, but the result was not reproducible.<sup>10</sup> On the other hand, the transformed crystalline peaks for the cube corner indentations observed in this study were seen consistently in each and every of ten separate indentations. Another important observation in Fig. 3(a) is how the crystalline phases diminish over time at room temperature and ambient pressure; after 20 h of aging, the peaks are barely discernible. This is consistent with the observations of Nelmes *et al.*,<sup>4</sup> who found using synchrotron x-ray diffraction that the Ge-IV phase formed in diamond anvil cell experiments vanishes within 17 h of removing the pressure.

Figure 3(b) presents the Raman spectra for indentations made under similar loading conditions with the Berkovich indenter. The spectra come from two separate indentations identified as Case A and Case B. Raman spectra exhibiting transformed crystalline phase (tentatively identified as Ge-IV above) and amorphous phase, such as those in Case B, were observed only occasionally. When observed, the peak intensities of the transformed phases were relatively low in comparison to those for the cube-corner indenter, and they diminished significantly after aging. The more common observation was Case A, in which only a shifted and broadened Ge-I peak is observed, with the shift indicating a compressive residual stress. It should be noted that even though the Raman spectra revealed transformed phases for Case B only, deformed zones—such as those shown within the con-

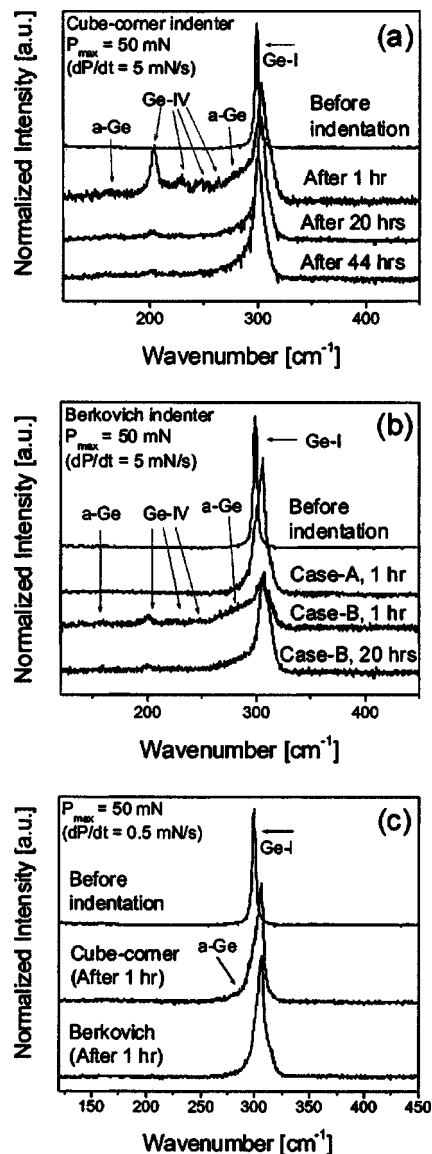


FIG. 3. Typical Raman spectra obtained from the center of the indents: (a) Cube-corner indentations,  $dP/dt=5$  mN/s, (b) Berkovich indentations,  $dP/dt=5$  mN/s, and (c) both cube-corner and Berkovich indentations,  $dP/dt=0.5$  mN/s.

tact impressions in Figs. 2(c) and 2(d)—were found for both Cases A and B.

Figure 3(c) shows the Raman spectra for cube-corner and Berkovich indentations performed at the slower loading/unloading rate of 0.5 mN/s. It is apparent that reducing the rate reduces the tendency to transform to metastable crystalline phases. The cube-corner indentation exhibits an asymmetry in the Ge-I peak which most likely indicates the presence of some amorphous Ge, but other than this, no transformation products could be identified. In contrast, slower unloading rates in diamond anvil cell experiments result in the formation of Ge-III (ST12). Olinyk and Jephcoat<sup>5</sup> have noted that Ge-III produced in diamond anvil experiments is very unstable under laser irradiation at ambient pressure and may transform to amorphous and Ge-I phases during micro-Raman characterization. We do not know if a similar phenomenon occurred in our examinations.

The observations reported here clearly indicate that phase transformations do indeed occur during the nanoindentation of germanium, but the transformations are reproduc-

ible only when sharper indenters are employed. This is most likely due to influences of indenter geometry on the contact mechanics. Because the cube-corner and Berkovich indenters give approximately the same indent size at a fixed load (see Fig. 2), the sharper cube-corner indenter displaces much more volume, thereby producing greater local pressures and shear stresses and a larger zone in which the stresses are high. Assuming the transformation from Ge-I to Ge-II during loading involves a nucleation and growth mechanism, the driving forces for transformation will thus be greater for the cube-corner indenter and the probability of transformation higher. For the Berkovich indenter, the observation that transformed phases are formed only occasionally indicates that the driving forces may not be sufficient to nucleate the transformation in the time periods involved in the experiment. In this case, plastic deformation must proceed by other mechanisms, such as twinning, as observed Bradby *et al.*,<sup>11</sup> and/or dislocation activity. In this sense, the indentation deformation of germanium involves a close interplay between competing deformation mechanisms, and which mechanism dominates depends on how fast each mechanism proceeds relative to the rate at which with stresses rise in the vicinity of the contact. An alternative explanation for the observed behavior is that the smaller transformed volume of material expected for the Berkovich indenter may more easily revert to Ge-I during unloading. Differences in the magnitudes of the shear stresses produced by the two indenters could also play an important role in the transformation, but this is not well understood.

This research was sponsored by the National Science Foundation under Grant No. DMR-0203552 (for three of the authors J.I.J., S.W., G.M.P.), and at the ORNL SHaRE User Center (for two authors M.J.L., G.M.P.) by the Division of Materials Sciences and Engineering, U.S. Department of Energy, under Contract No. DE-AC05-00OR22725 with UT-Battelle, LLC. The authors would like to thank Dr. V. Domnich for providing helpful documents.

- <sup>1</sup>J. C. Jamieson, *Science* **139**, 762 (1963).
- <sup>2</sup>R. J. Kobliska, S. A. Solin, M. Seiders, R. K. Chang, R. Alben, M. F. Thorpe, and D. Weaire, *Phys. Rev. Lett.* **29**, 725 (1972).
- <sup>3</sup>M. Hanfland and K. Syassen, *High Press. Res.* **3**, 242 (1990).
- <sup>4</sup>R. J. Nelmes, M. I. McMahon, N. G. Wright, D. R. Allan, and J. S. Loveday, *Phys. Rev. B* **48**, 9883 (1993).
- <sup>5</sup>H. Olinyk and A. P. Jephcoat, *Phys. Status Solidi B* **211**, 413 (1999).
- <sup>6</sup>V. Domnich and Y. Gogotsi, in *Handbook of Surfaces and Interfaces of Materials* Vol. 2, edited by H. S. Nalwa (Academic Press, New York, 2001), p. 355.
- <sup>7</sup>I. V. Gridneva, Y. V. Milman, and V. I. Trefilov, *Phys. Status Solidi A* **14**, 177 (1972).
- <sup>8</sup>D. R. Clarke, M. C. Kroll, P. D. Kirchner, and R. F. Cook, *Phys. Rev. Lett.* **60**, 2156 (1988).
- <sup>9</sup>A. Kailer, K. G. Nickel, and Y. G. Gogotsi, *J. Raman Spectrosc.* **30**, 939 (1999).
- <sup>10</sup>Y. G. Gogotsi, V. Domnich, S. N. Dub, A. Kailer, and K. G. Nickel, *J. Mater. Res.* **15**, 871 (2000).
- <sup>11</sup>J. E. Bradby, J. S. Williams, J. Wong-Leung, M. V. Swain, and P. Munroe, *Appl. Phys. Lett.* **80**, 2651 (2002).
- <sup>12</sup>J.-I. Jang, M. J. Lance, S. Wen, T. Y. Tsui, and G. M. Pharr, *Acta Mater.* **53**, 1759 (2005).
- <sup>13</sup>P. Lemaître, *J. Mater. Sci. Lett.* **7**, 895 (1988).
- <sup>14</sup>G. M. Pharr, W. C. Oliver, and D. S. Harding, *J. Mater. Res.* **6**, 1129 (1991).
- <sup>15</sup>S. V. Hainsworth, A. J. Whitehead, and T. F. Page, in *Plastic Deformation of Ceramics*, edited by R. C. Bradt, C. A. Brookes, and J. L. Routbort (Plenum, New York, 1995), p. 173.